Natural Convection in a Square Enclosure with a Circular Cylinder and Adiabatic Side Walls According to the Bottom Wall Temperature Variation

Myunggeun Jeong[a], Minsung Kim[a] and Man Yeong Ha[a]*
a School of Mechanical Engineering, Pusan National University, San 30, Jangjeon-dong, Geumjeong-gu, Busan 609-735, Korea
E-mail: hot4205@gmail.com

ABSTRACT

Two-dimensional numerical simulations are conducted for natural convection in an enclosure with a hot inner cylinder located at the center in the Rayleigh number range from 10^5 to 10^6. The Prandtl number is set to be 0.7 corresponding to the air. We investigate the effect of various temperature conditions on the bottom wall on thermal and flow structures of the natural convection in the enclosure. It is identified that the streamlines and isotherms in the enclosure depend on the Rayleigh number and the temperature condition imposed on the bottom wall of the enclosure. When Ra=10^5, small inner vortices are formed in the lower part of the cylinder and they show significant changes in their size due to the increase in the temperature on the bottom wall. When Ra=10^6, secondary vortices are formed in the lower part of the cylinder because of the separation of the main convection flow from the side walls. And the magnitude of the convection velocity at Ra=10^6 becomes much larger than that at Ra=10^5, which leads to the occurrence of a stronger upwelling plume above the top surface of the cylinder. The numerical solutions at Ra=10^5 reach the steady state after fully converged regardless of the variation in the temperature condition on the bottom wall. On the other hand, the numerical solutions for all cases at Ra=10^6 except the case with the temperature condition of zero show the time dependent characteristics.

INTRODUCTION

Natural convection in an enclosure is relevant to many practical applications such as heat exchangers, cooling of nuclear and chemical reactor systems, cooling of electronic equipment and so on. Due to various applications, fundamental studies on the natural convection in an enclosure, including Rayleigh-Bénard convection in a horizontal layer of the fluid confined between two parallel plates, have been performed by many researchers for decades [1-8].

Gelfat [1] described a complete numerical solution of the formulated benchmark problem devoted to the parametric study on Rayleigh-Bénard instability in rectangular two- and three-dimensional boxes. The results of the parametric calculations were presented in [1] as characteristic curves showing the dependence of the critical Rayleigh number on the aspect ratio of the cavity. Quertatani et al. [2] numerically performed a study on a classical Rayleigh-Bénard convection problem, and reported the characteristics of the flow and thermal structures for the Rayleigh numbers ranging from 10^3 to 10^6. D'Orazio et al. [3] studied the case of 2-D Rayleigh-Bénard convection developed in a cavity with a large aspect ratio ranging between 2 and 6, where the Rayleigh number range of $10^3 \sim 2\times10^6$ was considered in the study.

In many engineering applications, the situation frequently arises wherein diverse thermal boundary conditions are imposed on walls of an enclosure. Therefore, many studies have considered the effect of a thermal boundary condition on natural convection. Corcione [4] studied the natural convection

NOMENCLATURE

Symbols

f_i	[-]	Momentum forcing
g	[m/s^2]	Gravitational acceleration
h	[-]	Heat source or sink
H	[-]	Dimensionless vertical length of enclosure
L	[-]	Dimensionless horizontal length of enclosure
n	[-]	Direction normal to the wall
Nu	[-]	Nusselt number
P	[-]	Dimensionless pressure
Pr	[-]	Prandtl number
q	[-]	Mass source or sink
R	[-]	Dimensionless radius of circular cylinder
Ra	[-]	Rayleigh number
t	[-]	Dimensionless time
T	[K]	Temperature
u,v	[-]	Dimensionless velocity components in x and y directions
x,y	[-]	Cartesian coordinates

Special characters

α	[m^2/s]	Thermal diffusivity
β	[1/K]	Thermal expansion coefficient
δ_{ij}	[-]	Kronecker delta
ρ	[kg/m^3]	Density
ν	[m^2/s]	Kinematic viscosity
θ	[-]	Dimensionless temperature

Subscripts

b	Bottom wall
c	Cold
cyl	Cylinder
h	Hot
t	Top
$*$	Dimensional variable
$\langle\ \rangle$	Surface-averaged value

in an air-filled rectangular enclosure heated from below and cooled from above with respect to variable thermal boundary conditions imposed on the side walls. The author reported that bi-direction differential heating has a significant effect on the flow mode transition of natural convection in the horizontal cavity. Kim et al. [5] recently investigated the natural convection induced by a temperature difference between a cold outer square cylinder and a hot inner cylinder for different Rayleigh numbers in the range of 10^3 to 10^6. The location of an inner circular cylinder was changed vertically along the centerline of the square enclosure. They reported that the numerical solutions for the flow and thermal fields eventually reach the steady state for all Rayleigh numbers considered. The number, size, and formation of the convection cells strongly depended on the Rayleigh number and the position of the inner circular cylinder. Kandaswamy et al. [6] numerically studied unsteady laminar natural convection in an enclosure with partially-heated side walls and an inner body as an internal heat source. They investigated the effects of the aspect ratio of the enclosure, different Prandtl numbers, and locations of the thermally active part of the side walls. They described the flow structure and the heat distribution in the enclosure, and the profile of the convection velocity in the mid-plane of the enclosure, for various simulation parameters. In addition, they assessed the heat transfer rate from walls of the enclosure. Aydin and Yang [7] numerically investigated the natural convection in a square cavity with localized isothermal heating from below and symmetrical cooling from the side walls. They considered various lengths of the local heating zone as a main simulation parameter. They reported that the Nusselt number on the heated part of the bottom wall increases with increasing Rayleigh number and length of the heating zone. Lee et al. [8] numerically studied the effects of the locally heated bottom wall of the enclosure with an hot inner cylinder located at the center on thermal and flow structures of natural convection for different Rayleigh numbers in the range of 10^3 to 10^6. They reported that the numerical solutions for Rayleigh numbers ranging from 10^3 to 10^5 reach a steady state. On the other hand, at $Ra = 10^6$, thermal and flow fields show time-dependent characteristics after their full development. The generation and dissolution of vortices in the enclosure were dependent mainly on the size of the local heating zone. Basak et al. [9] studied effects of thermal boundary conditions in a square enclosure on buoyancy-induced convection flow with respect to fluids with different Prandtl numbers using the finite element method. They imposed a non-uniform heating conon the bottom wall. They reported that the non-uniform heating of the bottom wall produces a greater heat transfer rate in the center region of the bottom wall than that produced in the uniform heating case for the Rayleigh numbers considered.

Generally, natural convection in an enclosure, whose flow is caused by temperature-induced density variations, has been studied as mentioned above. It is relevant to many industrial and environment applications, such as heat exchanger, nuclear and chemical reactors, cooling of electronic equipment and stratified atmospheric boundary layers.

In this study, 2-D numerical simulations were performed for natural convection in a square enclosure with a hot inner circular cylinder in the range of Rayleigh numbers from 10^5 to 10^6 in order to compare the phenomena of the results which are studied by Lee et al. [8], academically. We investigated the effect of various temperature conditions of the bottom wall on the characteristics of the flow structure and heat transfer of natural convection.

NUMERICAL METHOD

A schematic of the system is shown in Fig. 1. The system consists of a square enclosure with length L and an inner circular cylinder with radius of R= 0.2 L which is located at the center of the enclosure. As shown in Fig. 1, the top wall is kept at a constant low temperature T_c. The bottom wall of the enclosure is kept at a constant temperature T_b whose value varies against the simulation case considered in this study. The adiabatic thermal boundary conditions are imposed on the side walls of the enclosure. The cylinder surface is kept at a constant high temperature T_h.

The governing equations describing unsteady incompressible viscous fluid flow and thermal fields are the continuity, momentum and energy conservation equations in their non-dimensional forms, which are defined as

$$\frac{\partial u_i}{\partial x_i} - q = 0 \tag{1}$$

$$\frac{\partial u_i}{\partial t} + u_j \frac{\partial u_i}{\partial x_j} = -\frac{\partial P}{\partial x_i} + Pr \frac{\partial^2 u_i}{\partial x_j \partial x_j} + RaPr\theta\delta_{i2} + f_i \tag{2}$$

$$\frac{\partial \theta}{\partial t} + u_j \frac{\partial \theta}{\partial x_j} = \frac{\partial^2 \theta}{\partial x_j \partial x_j} + h \tag{3}$$

where the dimensionless variables in Eqs. (1)-(3) are defined as follows:

$$t = \frac{t^* \alpha}{L^2},\ x_i = \frac{x_i^*}{L},\ u_i = \frac{u_i^* L}{\alpha},\ P = \frac{P^* L^2}{\rho \alpha^2},\ \theta = \frac{T^* - T_c^*}{T_h^* - T_c^*} \tag{4}$$

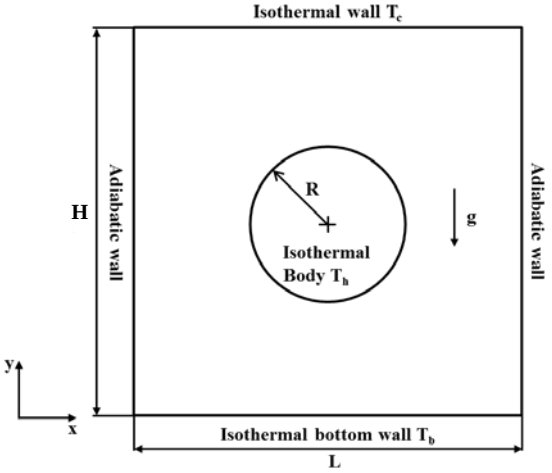

Figure 1 Computational domain and coordinate system along with boundary conditions

In Eq. (4), the superscript (*) denotes the dimensional variables; ρ and α represent the density and the thermal diffusivity of the fluid, respectively; P, θ, and t represent the dimensionless pressure, the dimensionless temperature, and the dimensionless time, respectively; x_i represents the dimensionless Cartesian coordinates; and u_i represents the corresponding dimensionless velocity components. Subscripts i and j are the tensor notation with i =1, 2 and j =1, 2. The fluid properties were assumed to be constant except in the buoyancy term according to the Boussinesq approximation which is only valid when temperature and, therefore, density variations are small. The aforementioned non-dimensionalization yields two dimensionless parameters: $\mathrm{Pr} = \nu/\alpha$ and $Ra = \dfrac{g\beta L^3(T_h - T_c)}{\nu\alpha}$, where ν, g, and β are the kinematic viscosity, gravitational acceleration and volume expansion coefficient, respectively. The gravitational acceleration g acts in the negative y direction. The Prandtl number was set to be $Pr = 0.7$ corresponding to the property of air. The Rayleigh numbers of 10^5 and 10^6 are considered in this study.

The immersed boundary method was used to capture the virtual surface boundary of the inner circular cylinder. The extra momentum forcing expressed by the term f_i in Eq. (2) is imposed at individual computational nodes inside the virtual boundary of the circular cylinder in order to comply with the wall no-slip boundary condition. The mass source/sink term q in Eq. (1) was applied on the cylinder surface or inside the cylinder to satisfy the mass conservation in the cell containing the virtual boundary. In Eq. (3), heat source/sink h was applied to satisfy the isothermal boundary condition on the virtual boundary. The four-step time-split scheme was used to advance the flow field.

For the flow field, no-slip and no-penetration boundary conditions were imposed on walls. For the temperature fields, the hot dimensionless temperature of $\theta_h = 1.0$ was imposed on the wall of the inner cylinder, whereas the cold dimensionless temperature of $\theta_c = 0.0$ was imposed on the top and side walls of the enclosure. For the bottom wall of the enclosure, the dimensionless temperature varies from $\theta_b = 0.0$ to $\theta_b = 1.0$ against the simulation case considered in this study.

Once the velocity and temperature fields were obtained, the local and surface-averaged Nusselt numbers were calculated as follows:

$$Nu = \left.\frac{\partial\theta}{\partial n}\right|_{wall}, \quad \langle Nu \rangle = \frac{1}{S}\int_0^S Nu\, ds \qquad (5)$$

where n is the direction normal to the wall and S the surface length.

The uniform grid is distributed in the computational domain as shown in Fig. 2. Table 1 shows the grid dependency test results when $Ra = 10^6$ and $\theta_b = 0.0$. As shown in Table 1, the difference in the values of surface-averaged Nusselt number on the cylinder, $\langle Nu_{cyl} \rangle$, calculated using different grid points of

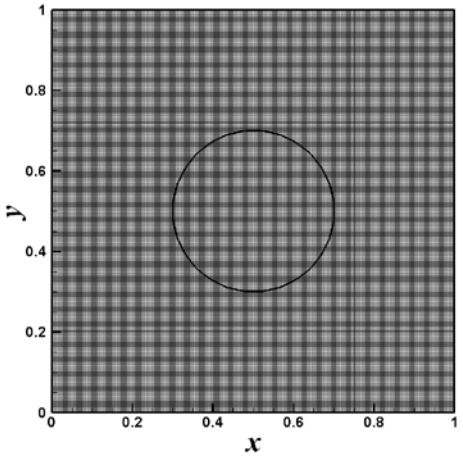

Figure 2 Distribution of the grid generated in the computational domain

Table 1 Grid dependency test results for the surface-averaged Nusselt number around the inner cylinder $\langle Nu_{cyl} \rangle$ when $Ra = 10^6$ and $\theta_b = 0.0$.

Grid number	$\langle Nu_{cyl} \rangle$	Difference (%)
202×202	4.9921	0.18
252×252	4.9902	0.21
302×302	4.9978	0.06
352×352	4.9998	0.02
402×402	5.0009	-

202×202, 252×252, 302×302, 352×352 and 402×402 for $Ra = 10^6$ and $\theta_b = 0.0$ is very small. Based on this grid dependency test result, a grid resolution of 302×302 along horizontal (x) and vertical (y) directions was employed in the present study.

RESULTS AND DISCUSSION

Figure 3(a) and 3(b) show distributions of isotherms and streamlines in the enclosure for cases of $\theta_b = 0.0$ at different Rayleigh numbers of 10^5 and 10^6, respectively. In terms of general fluid motion occurring due to natural convection as shown in Fig. 3, the heated lighter fluid is lifted along the hot surface of the inner cylinder due to buoyancy as a driving force. As the fluid flow approaches the cold top wall of the enclosure, it becomes gradually colder and denser. The fluid is cooled down further as it moves along the cold top wall in the lateral direction. Finally, a denser fluid cooled moves downward along adiabatic side walls of the enclosure. Thus, the main circulation of the convection flow is formed in the enclosure.

When $Ra = 10^5$, a single vortex core of each main circulation is located in the upper part of the cylinder, and a single upwelling plume can be identified above the top surface of the cylinder at $Ra = 10^5$ as shown in Fig. 3(a). When

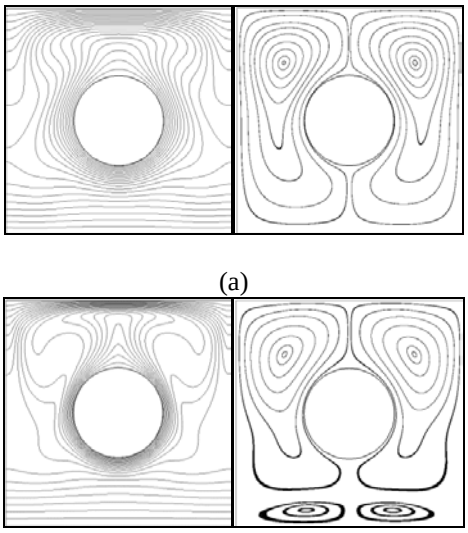

(a) (b)

Figure 3 Isothermals (left) and streamlines (right) distributed in the enclosure; (a) $Ra = 10^5$, (b) $Ra = 10^6$

$Ra = 10^6$, small secondary vortices occur in the vicinity of the bottom wall of the enclosure owing to the separation of the velocity boundary layer by the strong convective flow. Since the convection velocity significantly increases with increasing Rayleigh number, the thermal boundary layer behavior can be clearly observed around the cylinder and near the top wall of the enclosure as shown in isotherms of Fig. 3(b). The thermal boundary layer is lifted up from the top surface of the cylinder following a strong rising plume. The flow strongly impinges against the top wall of the enclosure, which leads to a thinner thermal boundary layer and thus the enhancement of the heat transfer capacity in this region.

Figure 4 shows the distribution of isotherms and streamlines

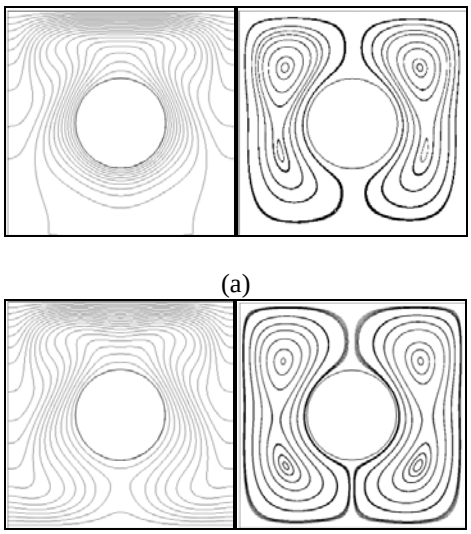

(a) (b)

Figure 4 Isothermals (left) and streamlines (right) distributed in the enclosure at $Ra = 10^5$ (a) $\theta_b = 0.5$, (b) $\theta_b = 1.0$

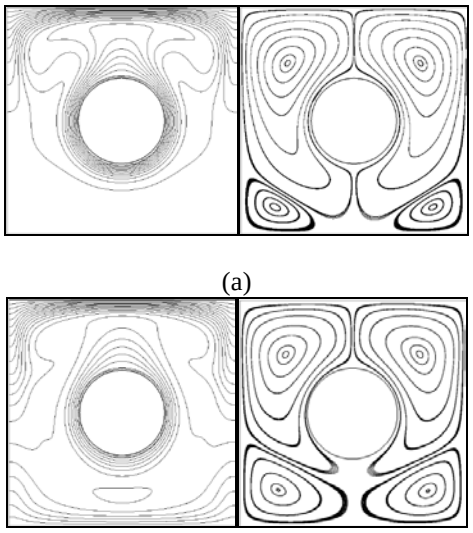

(a) (b)

Figure 5 Time-averaged isothermals (left) and streamlines (right) distributed in the enclosure at $Ra = 10^6$ (a) $\theta_b = 0.5$, (b) $\theta_b = 1.0$

at $Ra = 10^5$ according to the variation in θ_b. The numerical solutions at $Ra = 10^5$ reach the steady state regardless of the variation in the temperature condition on the bottom wall after fully converged. At $\theta_b = 0.5$ in Fig. 4(a), the bi-cellular vortical structure occurs in the main circulation flow. As θ_b increases to $\theta_b = 1.0$, lower inner vortices gradually increase in its size since the thermal gradient in the lower part of the cylinder is gradually stronger with increasing temperature of the bottom wall. As a result, the isotherms are distorted further as θ_b increases.

Figure 5 shows the distribution of time-averaged isotherms and streamlines at $Ra = 10^6$ according to the variation in θ_b. The numerical solutions for all cases at $Ra = 10^6$ except the case with the temperature condition of zero show the time dependent characteristics. When $\theta_b = 0.5$ in Fig. 5(a), secondary vortices are generated in the lower left and right corners of the enclosure, and their size increases gradually as θ_b increases. The primary vortices occupying most space in the enclosure are confined further to the upper region of the enclosure due to the presence of secondary vortices as the temperature on the bottom wall of the enclosure increases.

Figure 6 shows distributions of the surface-averaged Nusselt number on the cylinder surface $\langle Nu_{cyl} \rangle$, top wall $\langle Nu_t \rangle$ and bottom wall $\langle Nu_b \rangle$ of the enclosure as a function of θ_b for two different Rayleigh numbers considered in this study. In these figures, positive or negative values of the Nusselt number denote the direction of the heat transfer on walls. As shown in Fig. 6(a), the absolute value of $\langle Nu_{cyl} \rangle$ decreases monotonically with increasing θ_b at $Ra = 10^5$ and $Ra = 10^6$

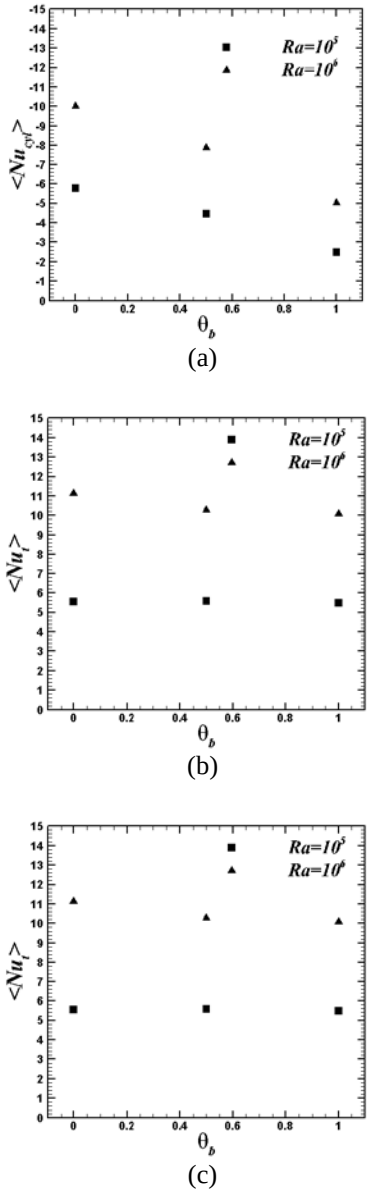

Figure 6 Time- and surface-averaged Nusselt for two different Rayleigh numbers; (a) cylinder surface, (b) top wall and (c) bottom wall of the enclosure

since the fluid temperature around the cylinder gradually increases with increasing θ_b . As shown in Fig. 6(b), the variation in $\langle Nu_t \rangle$ according to θ_b is very small for $Ra = 10^5$ and $Ra = 10^6$. At $Ra = 10^6$, the heat transfer rate is much larger than that at $Ra = 10^5$ due to effects of the strong convection and rising thermal plume impinging against the top surface of the enclosure. As shown in Fig. 6(c), $\langle Nu_b \rangle$ has positive values for $\theta_b = 0.0 \sim 0.5$ at $Ra = 10^5$, which means the heat transfer from the surrounding fluid to the bottom wall. The value of $\langle Nu_b \rangle$ at $Ra = 10^5$ gradually decreases with increasing θ_b from $\theta_b = 0.0$ to $\theta_b = 0.5$. After $\theta_b = 0.5$, the direction of the heat transfer is changed (i.e., a positive-to-negative Nusselt number), and then the absolute value of $\langle Nu_b \rangle$ gradually increases with increasing θ_b from 0.5 to 1.0. When $Ra = 10^6$, the variation trend in the $\langle Nu_b \rangle$ according to θ_b shows very similar to that at $Ra = 10^5$.

CONCLUSION

Two-dimensional numerical simulations are conducted for natural convection in an enclosure with a hot inner circular cylinder located at the center in the Rayleigh number range from 10^5 to 10^6 . We investigate the effect of various temperature conditions on the bottom wall on thermal and flow structures of the natural convection in the enclosure. It is identified that the streamlines and isotherms in the enclosure depend on the Rayleigh number and the temperature condition imposed on the bottom wall of the enclosure.

The numerical solutions at $Ra = 10^5$ reach the steady state regardless of the variation in the temperature condition on the bottom wall after fully converged. On the other hand, the numerical solutions for all cases at $Ra = 10^6$ except the case with the temperature condition of zero show the time dependent characteristics.

When $Ra = 10^5$, small inner vortices formed in the lower part of the cylinder show significant changes in their size due to the increase in the temperature on the bottom wall. When $Ra = 10^6$, secondary vortices are formed in the lower part of the cylinder due to the separation of the main convection flow from side walls of the enclosure.

When $Ra = 10^6$, much stronger rising plumes than those at $Ra = 10^5$ are formed above the top surface of the cylinder. Thinner thermal boundary layer is formed on the lower surface of the cylinder and the top surface of the enclosure due to the effects of the strong convection and rising thermal plume impinging against the top wall of the enclosure, which results in higher heat transfer capacity than that at $Ra = 10^5$.

ACKNOWLEDGEMENT

This work was supported by the National Research Foundation of Korea (NRF) grant funded by the Korea government(MSIP) (No. NRF-2013R1A2A2A01067251).

REFERENCES

[1] A. Y. Gelfgat, Different modes of Rayleigh–Bénard instability in two- and three-dimensional rectangular enclosures, *Journal of Computational Physics*, Vol. 156, 1999, pp. 300-324

[2] N. Quertatani, N. B. Cheikh, B. B. Beya and T. Lili, Numerical simulation of two-dimensional Rayleigh–Bénard convection in an enclosure, *Comptes Rendus Mecanique*, Vol.336, 2008, pp. 464-470

[3] M. C. D'Orazio, C. Cianfrini and M. Corcione, Rayleigh–Bénard convection in tall rectangular enclosures, *International Journal of Thermal Science*, Vol. 43, 2004, pp. 135-144
[4] M. Corcione, Effects of the thermal boundary conditions at the sidewalls upon natural convection in rectangular enclosures heated from below and cooled from above, *International Journal of Thermal Science*, Vol. 42, 2003, pp. 199-208
[5] B.S. Kim, D.S. Lee, M.Y. Ha and H.S. Yoon, A numerical study of natural convection in a square enclosure with a circular cylinder at different vertical locations, *International Journal of Heat and Mass Transfer*, Vol. 51, 2008, pp. 1888-1906
[6] P. Kandaswamy, N. Nithyadevi and C. O. Ng, Natural convection in enclosures with partially thermally active side walls containing internal heat sources, *Physics of Fluids*, Vol. 20 (9), 2008, pp. 097104-1-9
[7] O. Aydin and W. Yang, Natural convection in enclosures with localized heating from below and symmetrical cooling from sides, *International Journal of Numerical Methods for Heat and Fluid Flow*, Vol. 10 (5), 2000, pp. 518-529
[8] H.J. Lee, J.H. Doo, M.Y. Ha and H.S. Yoon, Effects of thermal boundary conditions on natural convection in a square enclosure with an inner circular cylinder locally heated from the bottom wall, *International Journal of Heat and Mass Transfer*, Vol. 65, 2013, pp.435-450
[9] T. Basak, S. Roy and A. R. Balakrishnan, Effect of thermal boundary condition on natural convection flows within a square cavity, *International Journal of Heat and Mass Transfer*, Vol. 49, 2006, pp. 4525-4535
[10] J. Kim, D. Kim, H. Choi, An immersed-boundary finite volume method for simulations of flow in complex geometries, *Journal of Computational Physics*, Vol.171, 2001, pp. 132-150
[11] C. Choi, M.Y. Ha and Y.G. Park, Characteristics of thermal convection in a rectangular channel with and inner cold circular cylinder, International Journal of Heat and Mass Transfer, Vol. 84, 2015, pp. 955-973
[12] J.R. Lee, M.Y. Ha, S. Balachandar, H.S. Yoon and S.S. Lee, Natural convection in a horizontal layer of fluid with a periodic array of square cylinders in the interior, *Physics of Fluids*, Vol. 16 (4), 2004, pp. 1097-1117
[13] H.S. Yoon, Y.G. Park and J.H. Jung, Natural convection in a square enclosure with differentially heated two horizontal cylinders, *Numerical Heat Transfer, Part A*, Vol. 65, 2014, pp. 305-326
[14] X. Xu, G. Sun, Z. Yu, Y. Hu, L. Fan and K. Cen, Numerical investigation of laminar natural convective heat transfer from a horizontal triangular cylinder to its concentric cylindrical enclosure, International Journal of Heat and Mass Transfer, Vol. 52, 2009, pp. 3176-3186
[15] A. D'Orazio and L. Fontana, Experimental study of free convection from a pair of vertical arrays of horizontal cylinders at very low Rayleigh numbers, *International Journal of Heat and Mass Transfer*, Vol. 53, 2010, pp. 3131-3142